BJR

https://doi.org/10.1259/bjr.20180642

Received: 20 July 2018 | Revised: 21 September 2018 | Accepted: 25 September 2018

Cite this article as:
O'Connor JPB, Robinson SP, Waterton JC. Imaging tumour hypoxia with oxygen-enhanced MRI and BOLD MRI. *Br J Radiol* 2019; **92**: 20180642.

REVIEW ARTICLE

Imaging tumour hypoxia with oxygen-enhanced MRI and BOLD MRI

[1,2]JAMES P B O'CONNOR, MA, PhD, FRCR, [3]SIMON P ROBINSON, PhD and [4,5]JOHN C WATERTON, MA, PhD, FRSC (UK)

[1]Division of Cancer Sciences, University of Manchester, Manchester, UK
[2]Department of Radiology, The Christie Hospital, Manchester, UK
[3]Division of Radiotherapy and Imaging, The Institute of Cancer Research, London, UK
[4]Division of Informatics, Imaging and Data Sciences, University of Manchester, Manchester, UK
[5]Bioxydyn Ltd., Manchester, UK

Address correspondence to: Dr James P B O'Connor
E-mail: *james.oconnor@manchester.ac.uk*

ABSTRACT

Hypoxia is known to be a poor prognostic indicator for nearly all solid tumours and also is predictive of treatment failure for radiotherapy, chemotherapy, surgery and targeted therapies. Imaging has potential to identify, spatially map and quantify tumour hypoxia prior to therapy, as well as track changes in hypoxia on treatment. At present no hypoxia imaging methods are available for routine clinical use. Research has largely focused on positron emission tomography (PET)-based techniques, but there is gathering evidence that MRI techniques may provide a practical and more readily translational alternative. In this review we focus on the potential for imaging hypoxia by measuring changes in longitudinal relaxation [R_1; termed oxygen-enhanced MRI or tumour oxygenation level dependent (TOLD) MRI] and effective transverse relaxation [R_2*; termed blood oxygenation level dependent (BOLD) MRI], induced by inhalation of either 100% oxygen or the radiosensitising hyperoxic gas carbogen. We explain the scientific principles behind oxygen-enhanced MRI and BOLD and discuss significant studies and their limitations. All imaging biomarkers require rigorous validation in order to translate into clinical use and the steps required to further develop oxygen-enhanced MRI and BOLD MRI into decision-making tools are discussed.

INTRODUCTION

Hypoxia occurs when the rate of oxygen delivery to tissue is inadequate to meet demand.[1] Disordered angiogenesis in tumours makes delivery inefficient, leading to hypoxia. This is a hallmark of cancer[2] and has been recognised for several decades as being a negative prognostic factor in most solid human cancers.[3–5] Furthermore, since the 1950s[6] hypoxia has been known to cause radioresistance, which results in failure in radiotherapy treatment.[7] More recently, tumour hypoxia has been implicated in the failure of chemotherapy regimens and numerous targeted therapies.[8]

In oncology there are three main approaches to circumventing these negative effects of tumour hypoxia. Modifiers such as carbogen gas (95%O_2:5%CO_2) and nicotinamide have been shown to alleviate tumour hypoxia in combination with existing (chemo)-radiotherapy,[9] through improving blood flow and tumour oxygenation. The hypoxic subregions within tumours can be targeted selectively, for example with hypoxia-activated prodrugs[10–12] or drugs that modify oxygen consumption.[13,14] Finally, there is interest in modulating the dose distribution of delivered radiation based on heterogeneity within tumours,[15] focusing on spatial differences in pathophysiological features such as glucose metabolism[16,17] as well as tissue hypoxia.[16,18]

Current clinical practice does not identify or quantify hypoxia in tumours. When patients present with cancer, their disease distribution and volume is initially staged.[19] Later, the change in these features following therapy is assessed by response monitoring.[20] However, these evaluations are based on anatomical and morphological staging and response systems that regard all abnormal tumour tissue as being equal in importance and relevance.[21] Various imaging methods are available that can take radiology beyond this approach and incorporate measurements of tumour function.[22] In this review, we discuss the various clinically available MRI methods that can map tumour hypoxia, with particular focus on oxygen-enhanced MRI [OE-MRI; also known as tumour oxygenation level dependent (TOLD) MRI and blood oxygenation dependent

Table 1. Summary of methods available to study hypoxia in the clinic. *e.g. [^{18}F]-fluoromisonidazole (FMISO), [^{18}F]-fluoroazomycinarabinoside (FAZA) or [^{18}F]-flortanidazole (HX4). **[^{64}Cu]-diacetyl-bis(N^4-methylthiosemicarbazone)

Technique	Invasive to tumour	Contrast agent requirements	Measured entity	Spatial resolution	Further comments
In vivo					
pO_2 histography	Yes	None	$[O_{2(s)}]$ inferred from rate of arrival of O_2 molecules at electrode	Sub mm scale	Very limited clinical availability
PET with [^{18}F]-labelled nitroimidazoles*	No	i.v. injection of tracer	Retained [^{18}F] or [^{64}Cu] implying insufficient $[O_2]$ to reverse effect of tissue reductases	Few mm scale except for rodent MRI 0.2 to 0.5 mm for rodent MRI	Some validation; limited availability
PET with [^{64}Cu] ATSM	No				Seldom used compared to [^{18}F] PET
DCE-MRI	No	i.v. injection of gadolinium-based contrast agent	Blood flow and permeability		Indirectly associated with hypoxia
R_1 weighted OE-MRI	No	Hyperoxic inhalation	$[O_{2(s)}]$		Emerging techniques requiring further validation
R_2* weighted BOLD MRI	No	optional hyperoxic inhalation	compartmentalised deoxyhaemoglobin		
Ex vivo					
Hypoxia RNA gene signatures	Yes	None	gene expression associated with hypoxia	μm scale	Requires tissue: provides important cross- validation for other hypoxia biomarkers
HIF 1α	Yes	None	HIF 1α transactivation		
GLUT 1 and CA-IX	Yes	None	HIF 1α transactivation		
Pimonidazole	Yes	Oral or i.v. administration	Retained nitroimidazole implying insufficient $[O_2]$ to reverse effect of tissue reductases		
Circulating osteopontin	No	None	Chronic hypoxia	N/A	

BOLD, blood oxygenation level dependent; DCE, dynamic contrast-enhanced ; OE, oxygen-enhanced; PET, positron emission tomography;RNA, ribonucleic acid.

(BOLD) MRI] and we critique the biomarkers derived from these methods.

REQUIREMENTS FOR A BIOMARKER OF HYPOXIA

A biomarker is a "defined characteristic that is measured as an indicator of normal biological processes, pathogenic processes or responses to an exposure or intervention, including therapeutic interventions".[23,24] Biomarkers are used in cancer medicine to diagnose, predict and to stratify patients into different treatment groups, and also to monitor response to therapy.[25]

For assessing hypoxia, biomarkers must be technically valid, shown to measure tumour biology and relate to clinical outcome.[26,27] Unfortunately at present, no biomarkers are used routinely to evaluate tumour hypoxia,[28] although several investigational approaches exist (Table 1). Oxygenation in tumours can be directly measured using needle electrodes, a technique that was invaluable in first proving the associations with hypoxia and treatment response using Eppendorf histography.[3,4,29,30] However, this technique was limited to accessible tumours and is not generally available.

Assessment of tissue-level hypoxia is common in pre-clinical experiments, but mapping the spatial distribution of hypoxic tumour tissue is also possible in humans. Strategies available use either exogenous administered compounds such as nitroimidazoles (*e.g.* pimonidazole) that bind to macromolecules in cells under hypoxic conditions,[31] or use endogenous markers such as proteins CA-IX and GLUT1.[32] Alternative approaches use gene signatures of hypoxia.[33] However, biopsies are challenging or impossible in some tumour types, provide only a limited subsampling of the tumour, and are difficult to interpret in the presence of temporally fluctuating hypoxia. Furthermore, repeat measurements are normally impractical.[28] In distinction, serological markers (*e.g.* osteopontin) have shown some utility[34] and can be performed on repeat sampling, but cannot distinguish levels of hypoxia in different tumours within the same patient.

Imaging is an attractive option since it can provide serial non-invasive sampling of whole tumour volumes. Imaging can both identify subregions within one tumour that vary in their hypoxic profiles, and simultaneously distinguish hypoxic and normoxic tumours from one another in the same patient.[15] At present no

MRI, positron emission tomography (PET) or other imaging biomarker has sufficient technical, biological and clinical validation to have been translated into routine clinical practice.[35] In the sections below, we review the current status of MRI biomarkers of hypoxia and discuss what further work is required to translate these techniques into clinical use.

MR CONTRAST MECHANISMS: POTENTIAL METHODS FOR IMAGING HYPOXIA

MRI is attractive as it offers several independent contrast mechanisms which interrogate different facets of hypoxia. In humans, MRI voxels are large (typically a few millimetres in each orthogonal dimension) in comparison with typically 0.1 mm distance between a hypoxic domain and its nearest capillary.[36] Although some subvoxel hypoxia heterogeneity can be expected, the resolution is more than adequate for radiotherapy planning. Registration of MRI with radiotherapy, however, is more difficult than for CT, single photon emission CT and PET, because of the different mechanisms of image formation.

Two substances of particular interest in imaging hypoxia are the dioxygen molecule, in solution, $O_{2(s)}$, which has two unpaired electrons[37] and the deoxyhaemoglobin monomer, Hb, which has four unpaired electrons. Both molecules have an effect on longitudinal relaxation rate (R_1), the reciprocal of the longitudinal relaxation time (T_1). Independently, the heterogeneous intravoxel distribution of Hb affects the effective transverse relaxation time (T_2*), through its effect on T_2' (Figure 1; details below). This effect on T_2* (unlike the effect on T_1) depends in a complex way on the spatial arrangement of the microvasculature and haematocrit, but in general higher concentrations of deoxyhaemoglobin in a voxel, are associated with short T_2*.

The unpaired electrons endow both substances with modest longitudinal relaxivities (r_1) at 1.5T of 0.17 $s^{-1}.mM^{-1}$ for $O_{2(s)}$ and 0.008 $s^{-1}.mM^{-1}$ for the Hb monomer.[38,39] These relaxivities and concentrations are too small to allow hypoxic tumours to be identified from their T_1 alone. However, switching the inhaled gas between air and 100% oxygen causes arterial hyperoxia. This in turn perturbs regional tumour concentrations of $O_{2(s)}$ and Hb imparting a heterogeneous change in R_1 (termed ΔR_1) which is directly related to tumour hypoxia. This experimental design is referred to as OE-MRI or TOLD contrast.[40,41]

Figure 1. Schematic representation of the change in R_1 and ΔR_2* induced by hyperoxic gas.

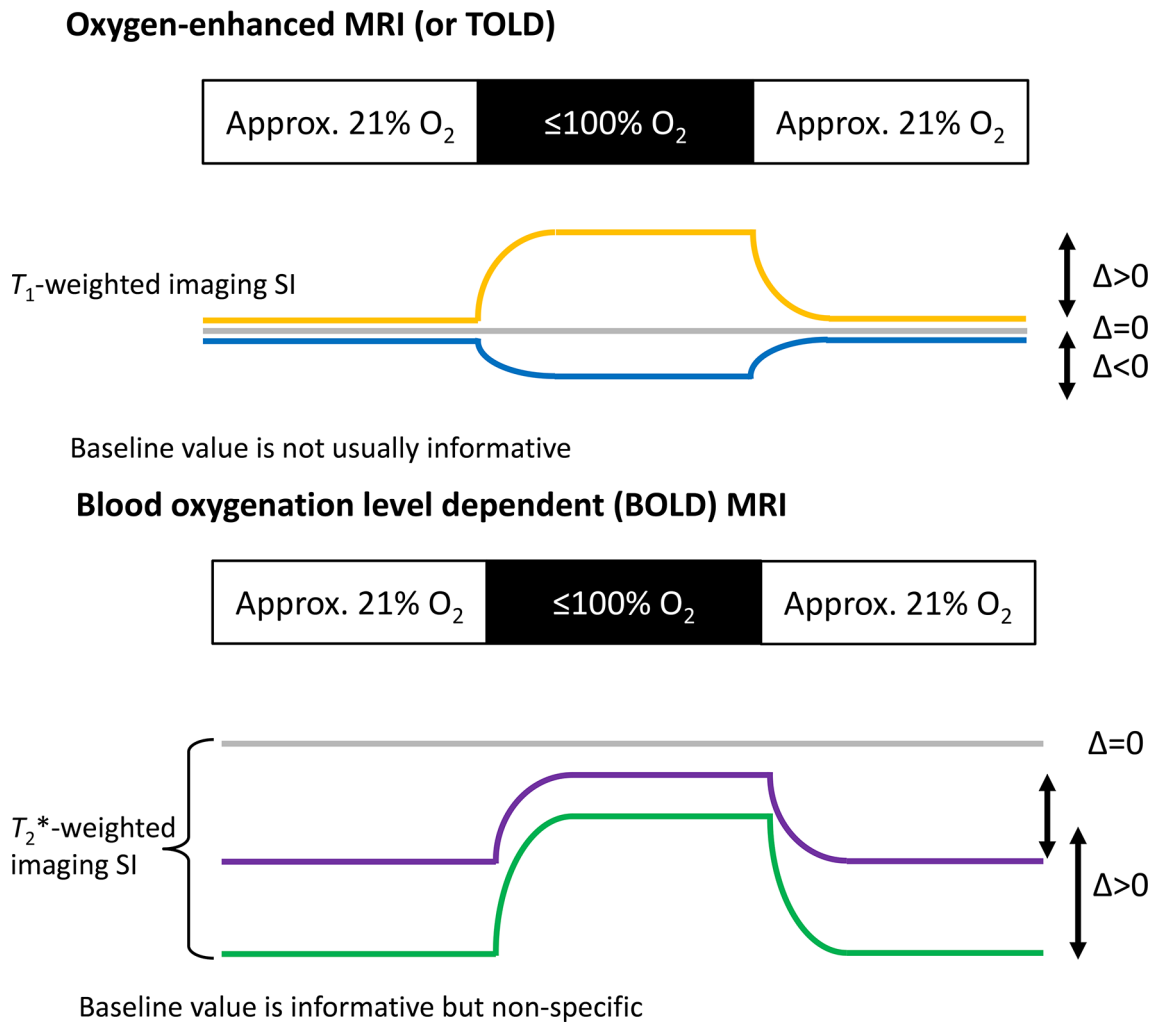

In addition to their longitudinal relaxivities, $O_{2(s)}$ and Hb make a paramagnetic contribution to tumour magnetic susceptibility which can be detected directly through susceptibility-weighted imaging.[42] The paramagnetic susceptibility of Hb has an additional and important use as it induces extreme field gradients around erythrocytes, massively enhancing signal dephasing and increasing the effective transverse relaxation rate (R_2*; reciprocal of T_2*)–the so-called BOLD effect.[43] However, rather than measure native R_2*, most studies exploit a similar experimental design to the above OE-MRI where the change in R_2* (termed ΔR_2*) is measured following perturbation with 100% oxygen. Unfortunately, unlike OE-MRI, there is no direct linear relationship between R_2* or hyperoxia-induced ΔR_2* and hypoxia.

An alternative experimental design uses carbogen gas as a hyperoxic challenge rather than 100% oxygen. This stems from the fact that many early BOLD studies were applied with the aim of measuring the effects of carbogen therapy. However, the interpretation of this design is more challenging because of the need to interpret the physiological effects of both O_2 and CO_2.[40] Studies in animal models and in humans have shown that the effects of the two gases differ between various normal tissues.[44,45] Furthermore, carbogen can be unpleasant to breathe. Because of these facts, and because most subsequent studies have not been designed to monitor the effect of carbogen as a therapy, many investigators have resorted to using 100% oxygen as a challenge instead of carbogen.

Other MRI biomarkers also provide indirect insight into hypoxia. Inadequate perfusion is a proximate cause of hypoxia and can be interrogated by arterial spin labelling or dynamic contrast-enhanced MRI (DCE-MRI).[46,47] Cell death and necrosis are a common consequence of hypoxia and can be reflected in elevated ADC or T_2.[22] Finally, a few investigational hypoxia-sensitive MRI probes have been used in pre-clinical studies, but have not progressed far in the clinic.[48,49]

OE-MRI: R_1 contrast MRI and hypoxia

In well-oxygenated voxels, inhaling excess O_2 increases R_1 because supply is already adequate to meet the demand of local mitochondria, and excess oxygen remains dissolved in blood plasma and interstitial tissue fluid.[50] The measured change, ΔR_1 induced by breathing oxygen is given by:

$$\triangle R1 = R_{1(t)} - R_{1(0)} = \triangle[O_2].r_{1,0_2} + \triangle[Hb].r_{1,Hb} \quad (1)$$

where $R_{1(0)}$ is R_1 at baseline, $R_{1(t)}$ is R_1 at time t after the switch to O_2 inhalation, depending on the changes in concentration of the two relaxive substances $\Delta[O_2]$ and Δ[Hb] together with their respective relaxivity constants $r_{1,O2}$ and $r_{1,Hb}$. The second, Hb-dependent, term is small and in many settings can be neglected, leaving ΔR_1 simply proportional to change in tissue oxygen concentration $\Delta[O_2]$. The R_1 values and concentrations are voxel-averages, R_1 is assumed to be mono-exponential and measurements are assumed not to be confounded by inflowing blood.

Multiple studies have shown that OE-MRI produces measurable signal changes in normal tissues and is feasible on both clinical scanners[40,51,52] and at the high field strengths used for pre-clinical studies,[45] with signal changes of up to 20% reported (Figure 2). Although the relaxivity of $O_{2(s)}$ declines at high field, this disadvantage is offset by the lower $R_{1(0)}$ and higher SNR at high field. The technique has also been used in several non-oncological settings over the last two decades in approximately 40 published studies of respiratory physiology and disease.[53–55]

Figure 2. OE-MRI in normal tissues: mean of the ΔR_1 recorded in the spleens of 16 healthy volunteers. There is a positive ΔR_1 induced following both 100% oxygen (O_2) and carbogen (CB), although the response seen with O_2 is slightly attenuated with CB gas. The ΔR_1 returns to baseline once air breathing is resumed. Adapted from reference.[40] OE-MRI, oxygen-enhanced MRI.

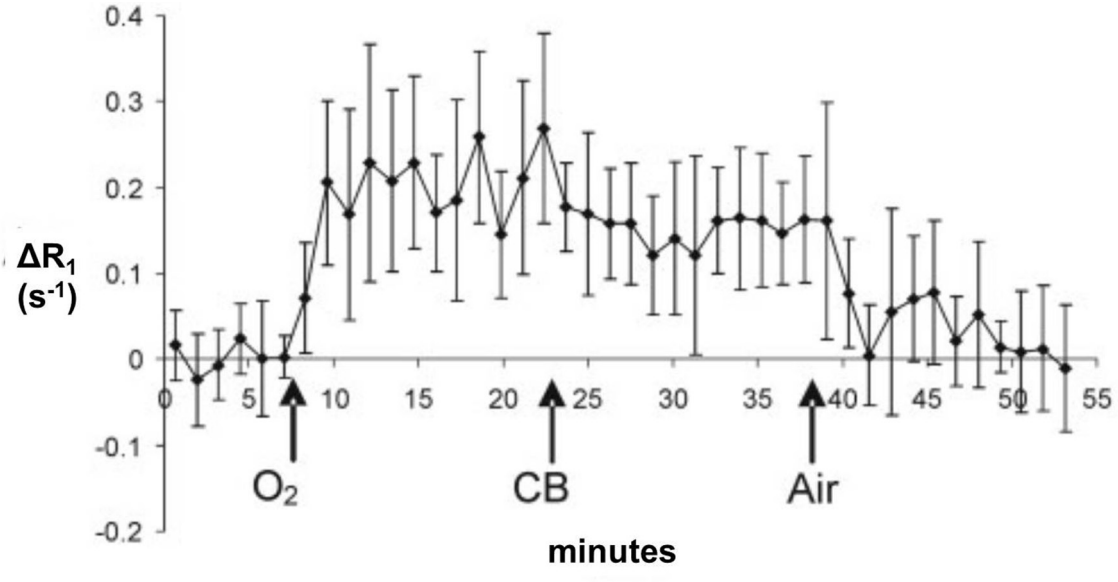

Since OE-MRI can measure oxygen delivery, investigators in the 2000s began to explore its role in oncology. In most studies of pre-clinical xenograft and orthotopic tumour models[41,56–62] and in some human tumors,[63–65] *positive* values of oxygen-induced ΔR_1 were reported, reflecting the average effect of O_2 inhalation in tumours. These studies covered a range of field strengths. R_1 changes, and the concomitant signal intensity changes in T_1-weighted MRI, are typically ≤5%, but with care the technique is feasible on both pre-clinical and clinical MRI platforms.

These studies of OE-MRI in oncology created interest in it being a method for use in studies of hypoxia. However, measuring *positive* ΔR_1 in OE-MRI quantifies and maps oxygen delivery in tissues with fully saturated haemoglobin, but does not directly identify tissue hypoxia *per se*. This inspired a second look at OE-MRI signal changes in tumours. For the first time, analyses highlighted that some tumour subregions were refractory in R_1 to oxygen challenge,[61,66] or even exhibited *negative* ΔR_1. These regions had low haemoglobin oxygen saturation, so excess O_2 molecules were immediately bound to Hb and did not significantly alter tissue $[O_{2(s)}]$.[28] At the same time this depletion of paramagnetic Hb may induce a barely-detectable decrease in R_1. Decreasing R_1 suggests a vascular volume fraction which is substantial (since only vasculature contains Hb), but nonetheless inadequate to supply the local mitochondria, perhaps because of chaotic architecture. Retrospective evaluation showed that this finding was also present in several other studies from other research groups.[41,56,61]

Based on these data, we investigated whether the regions that are perfused but lack oxygen enhancement (with an OE-MRI and DCE-MRI biomarker termed *perfused Oxy-R*) could identify hypoxic subregions within tumours.[31] This study showed for the first time the translational potential for OE-MRI,[36] since signals were accurate, precise, and sensitive to changes in tumour pO_2 (Figure 3A). The relationship of ΔR_1 to change in pO_2 has also been shown by another independent research group.[67] Furthermore, perfused Oxy-R fraction quantified the hypoxic fraction in multiple models and detected dynamic changes in hypoxia induced by a vasomodulator (Figure 3B).

The potential value of OE-MRI is now being investigated by several research groups. The method has been shown capable of distinguishing radiation necrosis from malignant high-grade glioma in mouse models[62] (Figure 4). This indicates a possible diagnostic application. The potential use in radiotherapy prognosis has been suggested in a small study of rats with Dunning R3327-AT1 tumours treated with radiotherapy, where those tumors with greater oxygen-induced ΔR_1 during therapy had greater growth delay.[68] In distinction, comparable results were not reported in mice bearing glioma and rhabdomyosarcoma xenografts where carbogen-induced challenges were

Figure 3. OE-MRI validation in tumours: (A) Positive increase in R_1 is induced following 100%oxygen (O_2) in a mouse model of renal carcinoma (786–0 R). OE-MRI changes are mirrored by change in tumour pO_2. (B) When OE-MRI signals are examined in perfused tissue, the oxygen refractory voxels (termed *perfused Oxy-R*; blue) are distinguished from oxygen-enhancing voxels (yellow); non-perfused voxels (grey) are excluded. The *perfused Oxy-R* fraction correlated significantly to the hypoxic volume measured on immunofluorescence.Adapted from reference.[31] OE-MRI, oxygen-enhanced MRI.

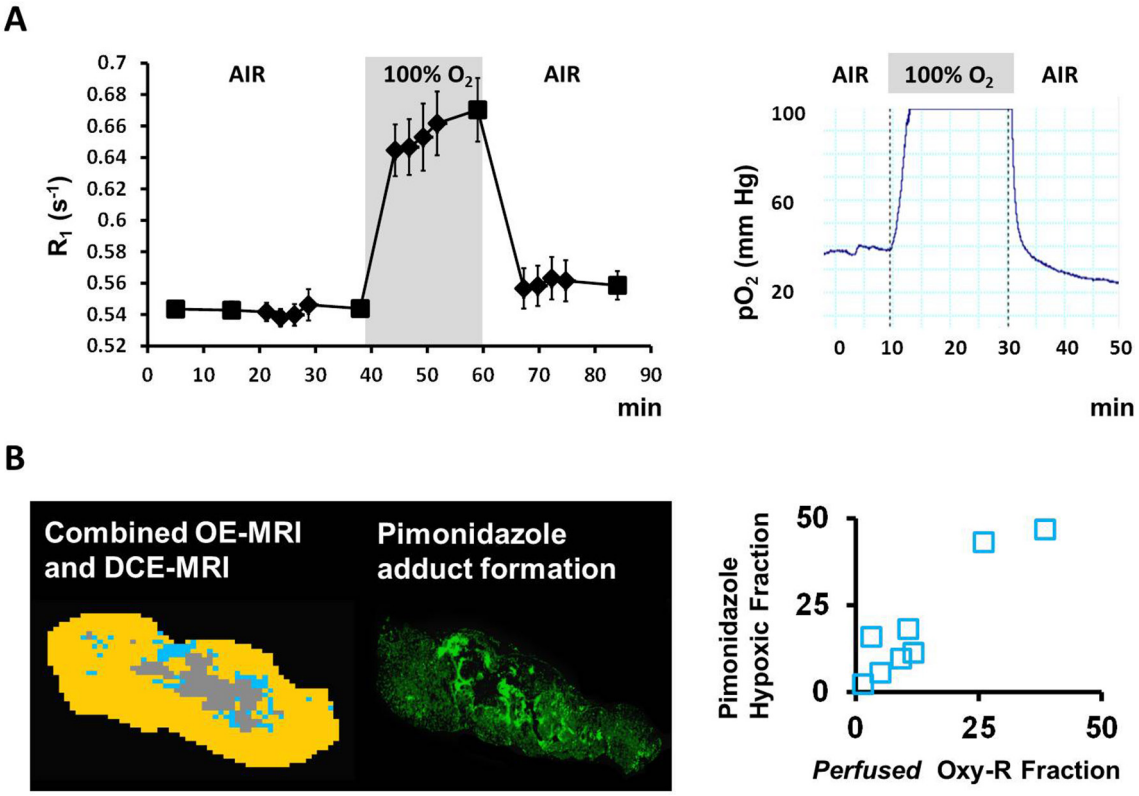

Figure 4. OE-MRI application: The ΔR_1 induced following carbogen inhalation distinguished tumour from radiation necrosis. Both pathologies had lower ΔR_1 than healthy brain in the contralateral hemisphere. Adapted from reference.[62] OE-MRI, oxygen-enhanced MRI.

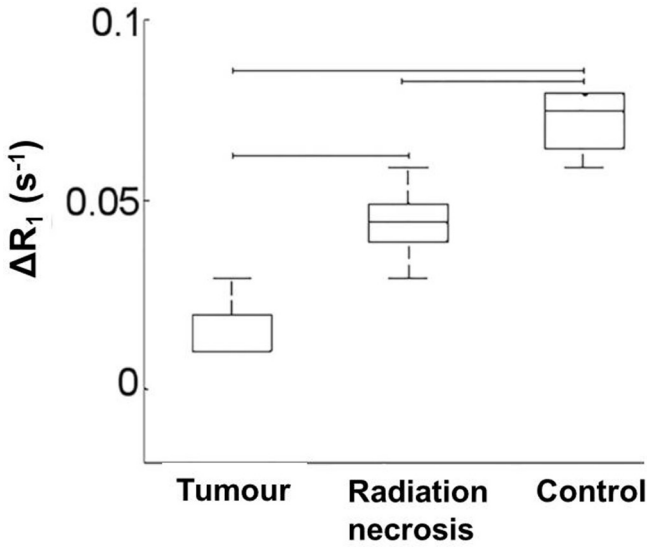

performed.[69] Further pre-clinical studies will be required to help determine the best clinical trial design to qualify the role of OE-MRI parameters as prognostic biomarkers.

Perhaps the most easily envisaged OE-MRI application may be in evaluating response to therapy. Although in their infancy, OE-MRI studies have shown considerable initial promise in this regard. A pre-clinical study using Calu6 and U87 xenografts has shown that the OE-MRI biomarker 'perfused Oxy-R' is sensitive to changes in hypoxia induced by hypoxia modifying targeted therapies.[70] Here, both the hypoxia-activated cytotoxic prodrug banoxantrone, and the oxygen consumption modifier atovaquone were shown to be active in the xenograft models, with reduction in the volume of tumor identified by OE-MRI, relative to control. Similarly, reduction in hypoxia has been shown with high-dose single fraction radiation as well as with fractionated chemoradiotherapy in the same xenograft models.[68,71]

BOLD: R_2* contrast MRI and hypoxia

The contribution of blood deoxyhaemoglobin to the R_2* relaxation rate of each voxel is not simple

$$\Delta R_2 = R_{2(t)} - R_{2(0)} = f\left(\Delta\left[Hb\right]\right) \quad (2)$$

Where f is an unknown non-linear function of the voxel dimensions and capillary geometry and Δ[Hb] is the change in tissue deoxyhaemoglobin concentration caused by hyperoxia.

Note that, unlike eq [1] for R_1, eq [2] is not a voxel-average, and the relationship between the relaxation rate and the concentration of the relaxive substance cannot be simply described by a relaxivity. ΔR_2* is determined by the vascular geometry, vascular volume and change in blood oxygenation, and may reflect the potential to enhance oxygen delivery to a tumour.

The oxygenation of haemoglobin depends on the arterial blood p_aO_2, but this is not in equilibrium with tissue pO_2 if viable mitochondria are present, because there must be an O_2 gradient from the vessels to the mitochondria. Measurements of tumour R_2* therefore cannot provide an index of tumour oxygenation. The relationship of R_2* weighted image response and tumour pO_2 has been investigated by invasive Eppendorf histography with carbogen breathing and showed a weak correlation.[72] A stronger correlation of carbogen-induced decreases in R_2* with tumour oxygen tension, measured by oxygen microelectrodes, has been observed in rat mammary carcinomas.[73] Carbogen-induced decreases in R_2* of rat intracranial gliomas were shown to correlate with an increase in pO_2 measured by EPR oximetry.[74] Simultaneous measurements of tumour R_2* and pO_2 have been achieved using an MRI-compatible fibre-optic pO_2 sensor.[75,76]

Collectively these studies demonstrated that the R_2* signal response to carbogen is temporally correlated with changes in tumour pO_2, but that there was no correlation between absolute R_2* and pO_2. Associations of tumour R_2* and oxygen-induced ΔR_2* with hypoxia and improved tumour oxygenation, measured using immunohistochemical detection of reduced 2-nitroimidazole adducts, have been demonstrated in a range of pre-clinical tumour models[77–80] (Figure 5). Taken together, these data suggest that BOLD MRI can be used to assess changes in tumour oxygenation and provide good evidence that a hyperoxia-induced decrease in R_2* is indicative of increased tumour oxygenation *in vivo*.[81]

As highlighted earlier, hyperoxia increases blood oxygenation, and the magnitude of the change in tumour R_2* is dependent on blood volume, which is itself a determinant of the hypoxic fraction.[82,83] BOLD MRI has been shown to correctly predict the relative effects of radiosensitisers on tumour hypoxic fraction.[84] One pre-clinical study sought to test the hypothesis that the baseline tumour R_2* and carbogen-induced ΔR_2* measured prior to radiotherapy were prognostic for treatment outcome. Prior to irradiation, tumour R_2* was quantified while the host breathed air and subsequently carbogen, and correlated with the subsequent tumour growth inhibition in response to ionizing radiation. Overall, tumours which exhibited a significantly faster baseline R_2* and a significantly greater carbogen-induced ΔR_2* were more responsive to radiotherapy (Figure 6).[85]

Despite potential distortion artefacts arising in the vicinity of air and tissue interfaces in some anatomical sites, BOLD MRI has been implemented on standard clinical scanners and good reproducibility of human tumour baseline R_2* maps demonstrated.[86] BOLD MRI has been used to quantify R_2* and carbogen-induced changes in R_2* of human head and neck cancers prior to radiotherapy.[87] In this study, all 11 patients studied showed a carbogen-induced tumour ΔR_2* (statistically significant in 7) prior to ARCON therapy, and subsequently showed a low tumour recurrence rate after a considerable follow-up time. A clinical study on hypoxia in prostate cancer compared

Figure 5. BOLD imaging validation in tumours: Parametric R_2* maps of a GH3 prolactinoma during inhalation of a) medical air and b) carbogen (CB). Intense (white) regions (relatively fast R_2*) in the initial air breathing reflect the presence of paramagnetic Hb, whilst dark areas (relatively slow R_2*) are consistent with the presence of oxyhaemoglobin. Inhalation of CB results in a clear decrease in R_2*, indicating a decrease in Hb. Composite fluorescence images showing the distribution of reduced 2-nitroimidazole adduct formation from c) CCI-103F (red), administered during air breathing, and d) pimonidazole (green), administered during CB breathing, obtained from the same GH3 tumour, are also shown. Spatially, both CCI-103F and pimonidazole adduct formation are co-localised, but the extent of hypoxia staining is reduced following CB, providing histopathological validation of carbogen-induced ΔR_2* as a non-invasive imaging biomarker of increased tumour oxygenation. BOLD, blood oxygenation level dependent.

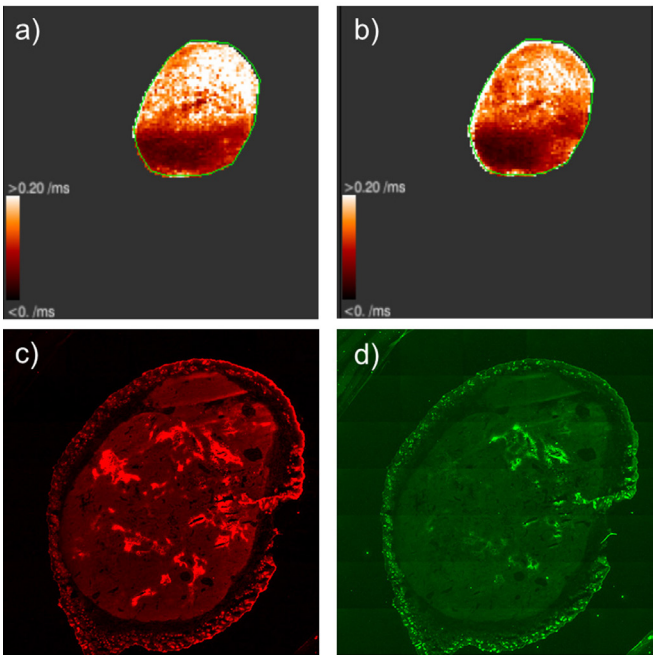

tumour R_2* and relative blood volume (rBV, measured by DCE MRI) with tissue sections immunohistochemically stained for pimonidazole.[88] Fast R_2* was correlated with pimonidazole staining and found to have a high sensitivity in depicting tumour hypoxia (88%), which was further enhanced by the addition of low rBV information (95%) without a change in specificity (36 and 29%, respectively), suggesting that the combination of native R_2* with rBV were effective in mapping intraprostatic tumour hypoxia. In a follow-up study, 17 patients with prostate cancer were investigated using R_2* measurements before and during a period of carbogen gas breathing.[89] 64% exhibited a reduction in tumour R_2* during carbogen inhalation, with a significant mean reduction of 22%, suggesting the presence of tumour hypoxia in the native state which was improved by carbogen inhalation. In exploring the relationship between BOLD MRI and invasive oxygen electrode measurements in human prostate cancer, a significant positive correlation was found between tumour R_2* and the fraction of tumour exhibiting pO_2 values < 5 mmHg, and a negative trend between R_2* and pO_2.[90]

Figure 6. BOLD imaging application: Pre-treatment R_2* and carbogen (CB)-induced ΔR_2* for individual GH3 prolactinomas (white triangles) and RIF-1 fibrosarcomas (black triangles), plotted against tumour volume at day 7 post-irradiation with 15 Gy as a percentage of the volume pre-treatment. GH3 prolactinomas displayed a fast baseline R_2*, large CB-induced ΔR_2* prior to radiotherapy and greater reduction in tumour volume post-irradiation. In contrast, RIF-1 fibrosarcomas displayed a slow baseline R_2*, negligible ΔR_2* response to CB and a smaller growth inhibition. The data suggest that quantitation of tumour R_2* and CB-induced ΔR_2* provide prognostic indicators of radiotherapeutic response. Adapted from reference.[85] BOLD, blood oxygenation level dependent.

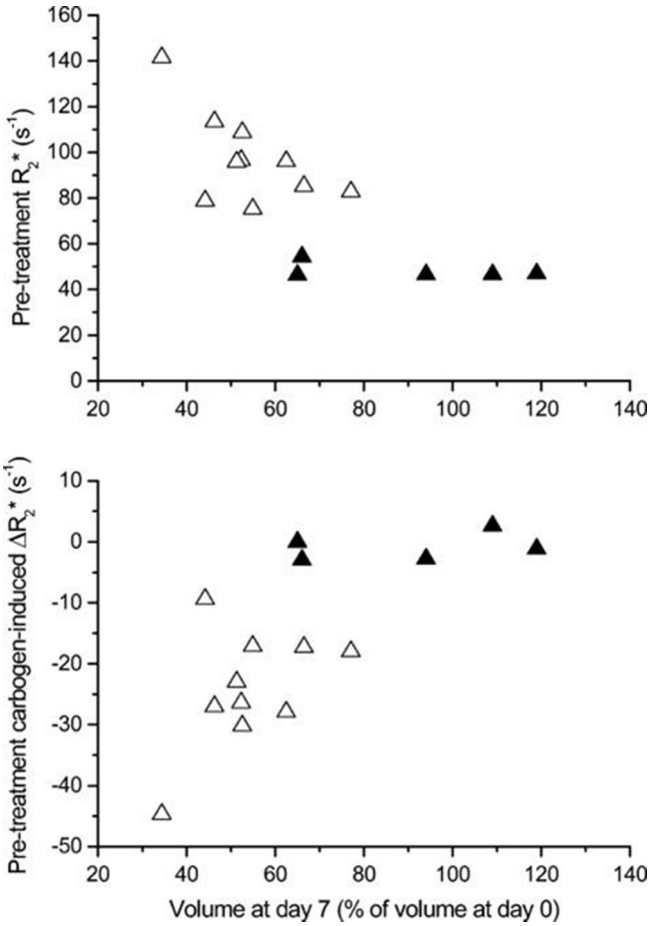

That said, opposite observations of R_2* values in relation to hypoxia have been observed in other tumour types. For example, in a pre-clinical study of mammary tumours, basal R_2* was negatively correlated with pimonidazole staining.[77] The relationship of native R_2* to tissue hypoxia appears to vary according to the underlying histology, and this relationship needs to be defined across a range of different tumour types.

Native R_2* and cycling hypoxia

Since the paramagnetic susceptibility of Hb induces extreme field gradients around erythrocytes it enhances signal dephasing and increases R_2*. Indeed, this effect is so pronounced that low tumour signal in T_2* weighted MRI suggests hypoxia. This effect has been exploited in a small number of studies, where the native

Figure 7. Native R_2* evaluation of cycling hypoxia: An example map of R_2* perturbation is shown of a lymph node metastasis from a patient with squamous cell head and neck cancer (with zoomed in section). An example of the power spectra tested for non-random fluctuations is shown. Adapted from reference.[96]

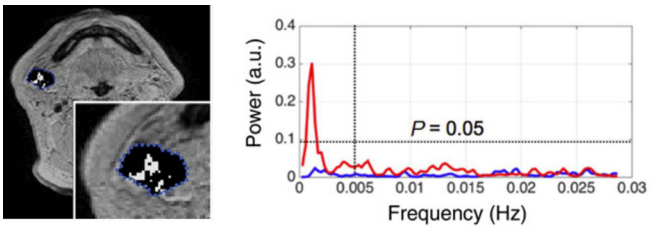

R_2* has been measured in the *absence of a challenge* with hyperoxic gas.

Cyclical hypoxia arises from fluctuations in erythrocyte flux through the abnormal tumour vasculature.[91–93] Given the sensitivity of R_2* to deoxygenated erythrocytes, continuous BOLD MRI measurements have been exploited pre-clinically to non-invasively image cyclical hypoxia through changes in the oxy/deoxyhaemoglobin ratio at high spatial and temporal resolution in both xenografts and patient tumours *in vivo*.[94–96] Frequencies in the range of 0.00027–0.001 Hz (corresponding to 15 to 60 min) were measured, comparable to the periodicity originally reported from classical pre-clinical invasive measurements of cyclical hypoxia.[97,98] Interestingly, in patients with head and neck squamous cell carcinoma, R_2* fluctuations spatially correlated with parts of lymph nodes with low K^{trans} values, typically in the vicinity of necrotic nodes. The R_2* fluctuation fraction was higher in the non-responding patient group, suggesting that the presence of such fluctuations may be predictive of a worse outcome following treatment for HNSCC[96] (Figure 7).

Comparison of R_1 and R_2* contrast MRI

Tumour subregions with low haemoglobin oxygen saturation are refractory to oxygen challenge on R_1 OE-MRI. Low haemoglobin oxygen saturation implies very low blood $[O_{2(s)}]$, and even lower tissue $[O_{2(s)}]$ if there are functional mitochondria. Even if oxygen challenge substantially increases haemoglobin oxygen saturation, the absolute changes in $[O_{2(s)}]$ are small, causing undetectable change in R_1. It is logical to suspect that the R_2* in these voxels should be high at baseline and also decrease on oxygen challenge because HbO_2, unlike Hb, causes no paramagnetic effect on magnetic susceptinility shift inside erythrocytes.

Several studies have examined the relationships between ΔR_1, native R_2* and ΔR_2* in xenografts[56–59,61] or in patient tumours.[65,99] These generally describe complex and non-linear relationships, possibly reflecting spatial or temporal heterogeneity with subregions of luxurious and inadequate perfusion present simultaneously and sometimes seen (with temporal disconnect) in the same voxel. However, potential confounds exist in both measurements; for example ΔR_1 can be confounded by inflow effects, ΔR_2* can be confounded by presence of haemorrhage and both parameters can be confounded by oxygen-induced vasoconstriction and by vascular steal (Figure 8).

Since it is unclear from these studies as to whether ΔR_1 and the R_2*-based biomarkers measure the same underlying tumour pathophysiology, we performed a study in a xenograft model and in seven patients with renal cell carcinoma to explore the

Figure 8. Schematic representation of the theoretical relationship between gas-induced ΔR_1 and ΔR_2*.

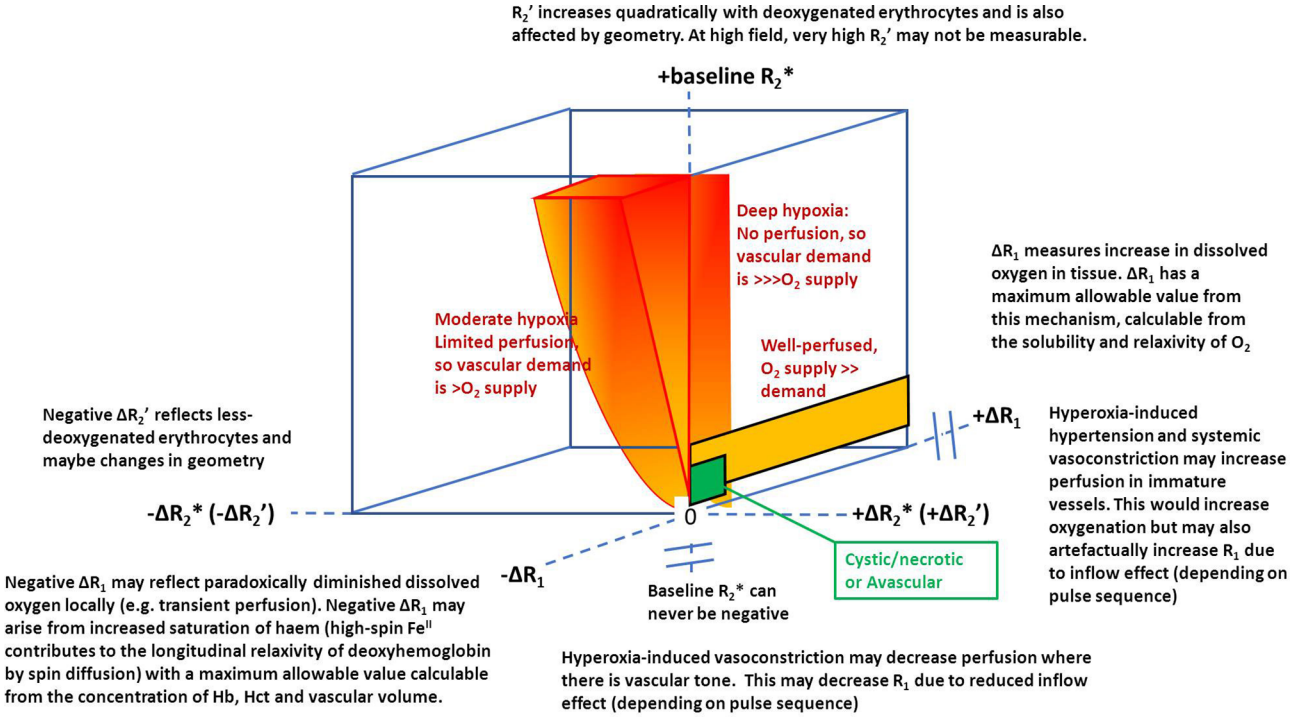

relationship between the two techniques.[80] Tumour-wise and voxel-wise ΔR_1 and ΔR_2^* comparisons did not show correlative relationships in 786–0 R renal cancer xenografts. However, parcellation analysis revealed that perfused Oxy-R regions had faster native R_2^* (102.4 s^{-1} vs 81.7 sec^{-1}) and greater negative ΔR_2^* (−22.9 s^{-1} *vs* −5.4 s^{-1}) when compared with perfused Oxy-E and non-perfused tumour subregions. Similar findings were present in human renal cell carcinomas.

FUTURE DIRECTIONS

Both R_1 and R_2^* gas-challenge MRI techniques have potential to identify, spatially map and quantify tumour hypoxia. There is a significant body of evidence that biomarkers derived from the two techniques can reflect underlying low pO_2 and resultant tissue hypoxia (identified by immunohistochemistry) in tumour subregions. However, nearly all of this data are in rodent tumour models and further investigation is required to add to the handful of small studies performed to date, to confirm that these findings are replicated consistently in a range of human cancer types. A small number of studies have also explored technical validation – such as repeatability – in a single centre setting. While these data are promising, further data are required to confirm high-to-excellent reproducibility in a multicentre setting using scanners that cover a range of vendors, MRI field strengths and sequences.[35]

However, the key questions for R_1 and R_2^* gas-challenge MRI will be to demonstrate readily measurable and consistent value of their biomarkers in clinical applications, such as identifying tumour hypoxia, tracking change in hypoxia on therapy or spatially mapping hypoxia to guide differential dose radiotherapy (dose painting).[100] This is an area of research priority for the next decade, which if successful could result in the rapid translation of these techniques into clinical decision making.

REFERENCES

1. Harris AL. Hypoxia-a key regulatory factor in tumour growth. *Nat Rev Cancer* 2002; **2**: 38–47. doi: https://doi.org/10.1038/nrc704
2. Hanahan D, Weinberg RA. Hallmarks of cancer: the next generation. *Cell* 2011; **144**: 646–74. doi: https://doi.org/10.1016/j.cell.2011.02.013
3. Hockel M, Schlenger K, Aral B, Mitze M, Schaffer U, Vaupel P. Association between tumor hypoxia and malignant progression in advanced cancer of the uterine cervix. *Cancer Res* 1996; **56**: 4509–15.
4. Brizel DM, Sibley GS, Prosnitz LR, Scher RL, Dewhirst MW. Tumor hypoxia adversely affects the prognosis of carcinoma of the head and neck. *Int J Radiat Oncol Biol Phys* 1997; **38**: 285–9. doi: https://doi.org/10.1016/S0360-3016(97)00101-6
5. Kroeger N, Seligson DB, Signoretti S, Yu H, Magyar CE, Huang J, et al. Poor prognosis and advanced clinicopathological features of clear cell renal cell carcinoma (ccRCC) are associated with cytoplasmic subcellular localisation of Hypoxia inducible factor-2α. *Eur J Cancer* 2014; **50**: 1531–40. doi: https://doi.org/10.1016/j.ejca.2014.01.031
6. Gray LH, Conger AD, Ebert M, Hornsey S, Scott OC. The concentration of oxygen dissolved in tissues at the time of irradiation as a factor in radiotherapy. *Br J Radiol* 1953; **26**: 638–48. doi: https://doi.org/10.1259/0007-1285-26-312-638
7. Nordsmark M, Bentzen SM, Rudat V, Brizel D, Lartigau E, Stadler P, et al. Prognostic value of tumor oxygenation in 397 head and neck tumors after primary radiation therapy. An international multi-center study. *Radiother Oncol* 2005; **77**: 18–24. doi: https://doi.org/10.1016/j.radonc.2005.06.038
8. Shannon AM, Bouchier-Hayes DJ, Condron CM, Toomey D. Tumour hypoxia, chemotherapeutic resistance and hypoxia-related therapies. *Cancer Treat Rev* 2003; **29**: 297–307. doi: https://doi.org/10.1016/S0305-7372(03)00003-3
9. Kaanders JH, Bussink J, van der Kogel AJ. ARCON: a novel biology-based approach in radiotherapy. *Lancet Oncol* 2002; **3**: 728–37. doi: https://doi.org/10.1016/S1470-2045(02)00929-4
10. Peeters SG, Zegers CM, Biemans R, Lieuwes NG, van Stiphout RG, Yaromina A, et al. TH-302 in combination with radiotherapy enhances the therapeutic outcome and is associated with pretreatment [18F]HX4 hypoxia PET imaging. *Clin Cancer Res* 2015; **21**: 2984–92. doi: https://doi.org/10.1158/1078-0432.CCR-15-0018
11. Wilson WR, Hay MP. Targeting hypoxia in cancer therapy. *Nat Rev Cancer* 2011; **11**: 393–410. doi: https://doi.org/10.1038/nrc3064
12. Phillips RM. Targeting the hypoxic fraction of tumours using hypoxia-activated prodrugs. *Cancer Chemother Pharmacol* 2016; **77**: 441–57. doi: https://doi.org/10.1007/s00280-015-2920-7
13. Ashton TM, Fokas E, Kunz-Schughart LA, Folkes LK, Anbalagan S, Huether M, et al. The anti-malarial atovaquone increases radiosensitivity by alleviating tumour hypoxia. *Nat Commun* 2016; **7**: 12308. doi: https://doi.org/10.1038/ncomms12308
14. Zannella VE, Pra AD, Muaddi H, McKee TD, Stapleton S, Sykes J, et al. Reprogramming Metabolism with Metformin Improves Tumor Oxygenation and Radiotherapy Response. *Cancer Res* 2013; **19**: 6741–50.
15. O'Connor JP, Rose CJ, Waterton JC, Carano RA, Parker GJ, Jackson A. Imaging intratumor heterogeneity: role in therapy response, resistance, and clinical outcome. *Clin Cancer Res* 2015; **21**: 249–57. doi: https://doi.org/10.1158/1078-0432.CCR-14-0990
16. Even AJ, van der Stoep J, Zegers CM, Reymen B, Troost EG, Lambin P, et al. PET-based dose painting in non-small cell lung cancer: Comparing uniform dose escalation with boosting hypoxic and metabolically active sub-volumes. *Radiother Oncol* 2015; **116**: 281–6. doi: https://doi.org/10.1016/j.radonc.2015.07.013
17. Aerts HJ, Bussink J, Oyen WJ, van Elmpt W, Folgering AM, Emans D, et al. Identification of residual metabolic-active areas within NSCLC tumours using a pre-radiotherapy FDG-PET-CT scan: a prospective validation. *Lung Cancer* 2012; **75**: 73–6. doi: https://doi.org/10.1016/j.lungcan.2011.06.003
18. Zschaeck S, Haase R, Abolmaali N, Perrin R, Stützer K, Appold S, et al. Spatial distribution of FMISO in head and neck squamous cell carcinomas during radio-chemotherapy and its correlation to pattern of failure. *Acta Oncol* 2015; **54**: 1355–63.

doi: https://doi.org/10.3109/0284186X.2015.1074720
19. Edge SB, Byrd DR, Compton CC, Fritz AG, Greene FL, Trotti A. *AJCC Cancer Staging Handbook*. 7th edition. New York: Springer; 2010.
20. Eisenhauer EA, Therasse P, Bogaerts J, Schwartz LH, Sargent D, Ford R, et al. New response evaluation criteria in solid tumours: revised RECIST guideline (version 1.1. *Eur J Cancer* 2009; **45**: 228–47. doi: https://doi.org/10.1016/j.ejca.2008.10.026
21. Michaelis LC, Ratain MJ. Measuring response in a post-RECIST world: from black and white to shades of grey. *Nat Rev Cancer* 2006; **6**: 409–14. doi: https://doi.org/10.1038/nrc1883
22. O'Connor JP, Jackson A, Asselin MC, Buckley DL, Parker GJ, Jayson GC. Quantitative imaging biomarkers in the clinical development of targeted therapeutics: current and future perspectives. *Lancet Oncol* 2008; **9**: 766–76. doi: https://doi.org/10.1016/S1470-2045(08)70196-7
23. .Biomarkers Definitions Working Group Biomarkers and surrogate endpoints: preferred definitions and conceptual framework. *Clin Pharmacol Ther* 2001; **69**: 89–95. doi: https://doi.org/10.1067/mcp.2001.113989
24. FDA-NIH Biomarker Working Group. BEST (Biomarkers, EndpointS, and other Tools) Resource. 2016. Available from: http://www.ncbi.nlm.nih.gov/books/NBK326791 [accessed 4th February 2016].
25. Parkinson DR, Johnson BE, Sledge GW. Making personalized cancer medicine a reality: challenges and opportunities in the development of biomarkers and companion diagnostics. *Clin Cancer Res* 2012; **18**: 619–24. doi: https://doi.org/10.1158/1078-0432.CCR-11-2017
26. Tatum JL, Kelloff GJ, Gillies RJ, Arbeit JM, Brown JM, Chao KS, et al. Hypoxia: importance in tumor biology, noninvasive measurement by imaging, and value of its measurement in the management of cancer therapy. *Int J Radiat Biol* 2006; **82**: 699–757. doi: https://doi.org/10.1080/09553000601002324
27. Salem A, Asselin M-C, Reymen B, Jackson A, Lambin P, West CML, et al. Targeting hypoxia to improve non–small cell lung cancer outcome. *JNCI: Journal of the National Cancer Institute* 2018; **110**: 14–30. doi: https://doi.org/10.1093/jnci/djx160
28. Hammond EM, Asselin M-C, Forster D, O'Connor JPB, Senra JM, Williams KJ. The Meaning, Measurement and Modification of Hypoxia in the Laboratory and the Clinic. *Clin Oncol* 2014; **26**: 277–88. doi: https://doi.org/10.1016/j.clon.2014.02.002
29. Okunieff P, Hoeckel M, Dunphy EP, Schlenger K, Knoop C, Vaupel P. Oxygen tension distributions are sufficient to explain the local response of human breast tumors treated with radiation alone. *Int J Radiat Oncol Biol Phys* 1993; **26**: 631–6. doi: https://doi.org/10.1016/0360-3016(93)90280-9
30. Gatenby RA, Kessler HB, Rosenblum JS, Coia LR, Moldofsky PJ, Hartz WH, et al. Oxygen distribution in squamous cell carcinoma metastases and its relationship to outcome of radiation therapy. *Int J Radiat Oncol Biol Phys* 1988; **14**: 831–8. doi: https://doi.org/10.1016/0360-3016(88)90002-8
31. O'Connor JP, Boult JK, Jamin Y, Babur M, Finegan KG, Williams KJ, et al. Oxygen-enhanced MRI accurately identifies, quantifies, and maps tumor hypoxia in preclinical cancer models. *Cancer Res* 2016; **76**: 787–95. doi: https://doi.org/10.1158/0008-5472.CAN-15-2062
32. Shannon AM, Telfer BA, Smith PD, Babur M, Logie A, Wilkinson RW, et al. The mitogen-activated protein/extracellular signal-regulated kinase kinase 1/2 inhibitor AZD6244 (ARRY-142886) enhances the radiation responsiveness of lung and colorectal tumor xenografts. *Clin Cancer Res* 2009; **15**: 6619–29. doi: https://doi.org/10.1158/1078-0432.CCR-08-2958
33. Buffa FM, Harris AL, West CM, Miller CJ. Large meta-analysis of multiple cancers reveals a common, compact and highly prognostic hypoxia metagene. *Br J Cancer* 2010; **102**: 428–35. doi: https://doi.org/10.1038/sj.bjc.6605450
34. Overgaard J, Eriksen JG, Nordsmark M, Alsner J, Horsman MR, .Danish Head and Neck Cancer Study Group Plasma osteopontin, hypoxia, and response to the hypoxia sensitiser nimorazole in radiotherapy of head and neck cancer: results from the DAHANCA 5 randomised double-blind placebo-controlled trial. *Lancet Oncol* 2005; **6**: 757–64. doi: https://doi.org/10.1016/S1470-2045(05)70292-8
35. O'Connor JPB, Aboagye EO, Adams JE, Aerts H, Barrington SF, Beer AJ. Imaging Biomarker Roadmap for Cancer Studies Nat Rev Clin Oncol. 2017; **14**: 169–86.
35. Dewhirst MW, Birer SR. Oxygen-enhanced MRI Is a major advance in tumor hypoxia imaging. *Cancer Res* 2016; **76**: 769–72. doi: https://doi.org/10.1158/0008-5472.CAN-15-2818
37. Young IR, Clarke GJ, Bailes DR, Pennock JM, Doyle FH, Bydder GM. Enhancement of relaxation rate with paramagnetic contrast agents in NMR imaging. *J Comput Tomogr* 1981; **5**: 543–7. doi: https://doi.org/10.1016/0149-936X(81)90089-8
38. Blockley NP, Jiang L, Gardener AG, Ludman CN, Francis ST, Gowland PA. Field strength dependence of R1 and R2* relaxivities of human whole blood to ProHance, Vasovist, and deoxyhemoglobin. *Magn Reson Med* 2008; **60**: 1313–20. doi: https://doi.org/10.1002/mrm.21792
39. Hales PW, Kirkham FJ, Clark CA. A general model to calculate the spin-lattice (T1) relaxation time of blood, accounting for haematocrit, oxygen saturation and magnetic field strength. *J Cereb Blood Flow Metab* 2016; **36**: 370–4. doi: https://doi.org/10.1177/0271678X15605856
40. O'Connor JP, Jackson A, Buonaccorsi GA, Buckley DL, Roberts C, Watson Y, et al. Organ-specific effects of oxygen and carbogen gas inhalation on tissue longitudinal relaxation times. *Magn Reson Med* 2007; **58**: 490–6. doi: https://doi.org/10.1002/mrm.21357
41. Zhao D, Pacheco-Torres J, Hallac RR, White D, Peschke P, Cerdan S, et al. Dynamic oxygen challenge evaluated by NMR T1 and T2 * - insights into tumor oxygenation. *NMR Biomed* 2015; **28**: 937–47.
42. Karczmar GS, River JN, Li J, Vijayakumar S, Goldman Z, Lewis MZ. Effects of hyperoxia onT2* and resonance frequency weighted magnetic resonance images of rodent tumours. *NMR Biomed* 1994; **7**(1-2): 3–11. doi: https://doi.org/10.1002/nbm.1940070103
43. Thulborn KR, Waterton JC, Matthews PM, Radda GK. Oxygenation dependence of the transverse relaxation time of water protons in whole blood at high field. *Biochimica et Biophysica Acta (BBA) - General Subjects* 1982; **714**: 265–70. doi: https://doi.org/10.1016/0304-4165(82)90333-6
44. O'Connor JP, Naish JH, Jackson A, Waterton JC, Watson Y, Cheung S, et al. Comparison of normal tissue R1 and R*2 modulation by oxygen and carbogen. *Magn Reson Med* 2009; **61**: 75–83.
45. Winter JD, Estrada M, Cheng HL. Normal tissue quantitative T1 and T2* MRI relaxation time responses to hypercapnic and hyperoxic gases. *Acad Radiol* 2011; **18**: 1159–67. doi: https://doi.org/10.1016/j.acra.2011.04.016
46. O'Connor JPB, Tofts PS, Miles KA, Parkes LM, Thompson G, Jackson A. Dynamic contrast-enhanced imaging techniques: CT and MRI. *Br J Radiol* 2011; **842** :: S112–S120Spec No. doi: https://doi.org/10.1259/bjr/55166688
47. Egeland TAM, Gaustad J-V, Vestvik IK, Benjaminsen IC, Mathiesen B, Rofstad EK.

Assessment of fraction of radiobiologically hypoxic cells in human melanoma xenografts by dynamic contrast-enhanced MRI. *Magn Reson Med* 2006; **55**: 874–82. doi: https://doi.org/10.1002/mrm.20852
48. Lee CP, Payne GS, Oregioni A, Ruddle R, Tan S, Raynaud FI, et al. A phase I study of the nitroimidazole hypoxia marker SR4554 using 19F magnetic resonance spectroscopy. *Br J Cancer* 2009; **101**: 1860–8. doi: https://doi.org/10.1038/sj.bjc.6605425
49. Shi Y, Oeh J, Eastham-Anderson J, Yee S, Finkle D, Peale FV, et al. Mapping in vivo tumor oxygenation within viable tumor by 19F-MRI and multispectral analysis. *Neoplasia* 2013; **15**: 1241–50. doi: https://doi.org/10.1593/neo.131468
50. Gray LH, Steadman JM. Determination of the oxyhaemoglobin dissociation curves for mouse and rat blood. *J Physiol* 1964; **175**: 161–71. doi: https://doi.org/10.1113/jphysiol.1964.sp007509
51. Tadamura E, Hatabu H, Li W, Prasad PV, Edelman RR. Effect of oxygen inhalation on relaxation times in various tissues. *Journal of Magnetic Resonance Imaging* 1997; **7**: 220–5. doi: https://doi.org/10.1002/jmri.1880070134
52. Jones RA, Ries M, Moonen CTW, Grenier N. Imaging the changes in renalT1 induced by the inhalation of pure oxygen: A feasibility study. *Magn Reson Med* 2002; **47**: 728–35. doi: https://doi.org/10.1002/mrm.10127
53. Edelman RR, Hatabu H, Tadamura E, Li W, Prasad PV. Noninvasive assessment of regional ventilation in the human lung using oxygen–enhanced magnetic resonance imaging. *Nat Med* 1996; **2**: 1236–9. doi: https://doi.org/10.1038/nm1196-1236
54. Ohno Y, Koyama H, Nogami M, Takenaka D, Matsumoto S, Obara M, et al. Dynamic oxygen-enhanced MRI versus quantitative CT: pulmonary functional loss assessment and clinical stage classification of smoking-related COPD. *American Journal of Roentgenology* 2008; **190**: W93–W99. doi: https://doi.org/10.2214/AJR.07.2511
55. Morgan AR, Parker GJM, Roberts C, Buonaccorsi GA, Maguire NC, Hubbard Cristinacce PL, et al. Feasibility assessment of using oxygen-enhanced magnetic resonance imaging for evaluating the effect of pharmacological treatment in COPD. *Eur J Radiol* 2014; **83**: 2093–101. doi: https://doi.org/10.1016/j.ejrad.2014.08.004
56. Matsumoto K-ichiro, Bernardo M, Subramanian S, Choyke P, Mitchell JB, Krishna MC, et al. MR assessment of changes of tumor in response to hyperbaric oxygen treatment. *Magn Reson Med* 2006; **56**: 240–6. doi: https://doi.org/10.1002/mrm.20961
57. Winter JD, Akens MK, Cheng H-LM. Quantitative MRI assessment of VX2 tumour oxygenation changes in response to hyperoxia and hypercapnia. *Phys Med Biol* 2011; **56**: 1225–42. doi: https://doi.org/10.1088/0031-9155/56/5/001
58. Burrell JS, Walker-Samuel S, Baker LC, Boult JK, Jamin Y, Halliday J, et al. Exploring ΔR2* and ΔR1 as imaging biomarkers of tumor oxygenation. *J Magn Reson Imaging* 2013; **38**: 429–34.
59. Jordan BF, Magat J, Colliez F, Ozel E, Fruytier A-C, Marchand V, et al. Mapping of oxygen by imaging lipids relaxation enhancement: A potential sensitive endogenous MRI contrast to map variations in tissue oxygenation. *Magn Reson Med* 2013; **70**: 732–44. doi: https://doi.org/10.1002/mrm.24511
60. Colliez F, Neveu M-A, Magat J, Cao Pham TT, Gallez B, Jordan BF. Qualification of a noninvasive magnetic resonance imaging biomarker to assess tumor oxygenation. *Clinical Cancer Research* 2014; **20**: 5403–11. doi: https://doi.org/10.1158/1078-0432.CCR-13-3434
61. Hallac RR, Zhou H, Pidikiti R, Song K, Stojadinovic S, Zhao D, et al. Correlations of noninvasive BOLD and TOLD MRI with pO_2 and relevance to tumor radiation response. *Magn Reson Med* 2014; **71**: 1863–73. doi: https://doi.org/10.1002/mrm.24846
62. Beeman SC, Shui Y-B, Perez-Torres CJ, Engelbach JA, Ackerman JJH, Garbow JR. O_2 -sensitive MRI distinguishes brain tumor versus radiation necrosis in murine models. *Magn Reson Med* 2016; **75**: 2442–7. doi: https://doi.org/10.1002/mrm.25821
63. Arnold JF, Kotas M, Fidler F, Pracht ED, Flentje M, Jakob PM. Quantitative regional oxygen transfer imaging of the human lung. *J Magn Reson Imaging* 2007; **26**: 637–45. doi: https://doi.org/10.1002/jmri.21033
64. O'Connor JPB, Naish JH, Parker GJM, Waterton JC, Watson Y, Jayson GC, et al. Preliminary study of oxygen-enhanced longitudinal relaxation in MRI: a potential novel biomarker of oxygenation changes in solid tumors. *Int J Radiat Oncol Biol Phys* 2009; **75**: 1209–15. doi: https://doi.org/10.1016/j.ijrobp.2008.12.040
64. Remmele S, Sprinkart AM, Müller A, Träber F, von Lehe M, Gieseke J, et al. Dynamic and simultaneous MR measurement of R1 and R2* changes during respiratory challenges for the assessment of blood and tissue oxygenation. *Magn Reson Med* 2013; **70**: 136–46. doi: https://doi.org/10.1002/mrm.24458
66. Linnik IV, Scott MLJ, Holliday KF, Woodhouse N, Waterton JC, O'Connor JPB, et al. Noninvasive tumor hypoxia measurement using magnetic resonance imaging in murine U87 glioma xenografts and in patients with glioblastoma. *Magn Reson Med* 2014; **71**: 1854–62. doi: https://doi.org/10.1002/mrm.24826
67. Cao-Pham TT, Joudiou N, Van Hul M, Bouzin C, Cani PD, Gallez B, et al. Combined endogenous MR biomarkers to predict basal tumor oxygenation and response to hyperoxic challenge. *NMR Biomed* 2018; **31**.
68. White DA, Zhang Z, Li L, Gerberich J, Stojadinovic S, Peschke P, et al. Developing oxygen-enhanced magnetic resonance imaging as a prognostic biomarker of radiation response. *Cancer Lett* 2016; **380**: 69–77. doi: https://doi.org/10.1016/j.canlet.2016.06.003
69. Cao-Pham TT, Tran LB, Colliez F, Joudiou N, El Bachiri S, Grégoire V, et al. Tumor response to carbogen breathing by oxygen-sensitive magnetic resonance parameters to predict the outcome of radiation therapy: a preclinical study. *Int J Radiat Oncol Biol Phys* 2016; **96**: 149–60. doi: https://doi.org/10.1016/j.ijrobp.2016.04.029
70. Little RA, Tessyman V, Babur M, Cheung S, Watson Y, Gieling R, et al. In vivo OE-MRI quantification and mapping of response to hypoxia modifying drugs Banoxantrone and Atovaquone in Calu6 xenografts. *Proceedings ISMRM* 2017; **25**: 2919.
71. Salem A, Little RA, Featherstone AK, Cheung S, Watson Y, Matthews J. Oxygen-enhanced MRI is feasible, repeatable and detects radiotherapy induced NSCLC hypoxia changes. *ESTRO* 2018; **37**.
72. Robinson SP, Collingridge DR, Howe FA, Rodrigues LM, Chaplin DJ, Griffiths JR. Tumour response to hypercapnia and hyperoxia monitored by FLOOD magnetic resonance imaging. *NMR Biomed* 1999; **12**: 98–106. doi: https://doi.org/10.1002/(SICI)1099-1492(199904)12:2<98::AID-NBM556>3.0.CO;2-I
73. Al-Hallaq H, River J, Zamora M, Oikawa H, Karczmar G. Correlation of magnetic resonance and oxygen microelectrode measurements of carbogen-induced changes in tumor oxygenation. *Int J Radiat Oncol Biol Phys* 1998; **41**: 151–9. doi: https://doi.org/10.1016/S0360-3016(98)00038-8
74. Dunn JF, O'Hara JA, Zaim-Wadghiri Y, Lei H, Meyerand ME, Grinberg OY, et al. Changes in oxygenation of intracranial tumors with carbogen: a BOLD MRI and

EPR oximetry study. *J Magn Reson Imaging* 2002; **16**: 511–21. doi: https://doi.org/10.1002/jmri.10192
75. Baudelet C, Gallez B. How does blood oxygen level-dependent (BOLD) contrast correlate with oxygen partial pressure (pO_2) inside tumors? *Magn Reson Med* 2002; **48**: 980–6. doi: https://doi.org/10.1002/mrm.10318
76. Robinson SP. Blood oxygenation level dependent (BOLD) imaging of tumours. In: eds.*Padhani AR, Choyke PL*. Boca Raton: New Techniques in Oncologic ImagingTaylor & Francis; 2006. pp. 257–72.
77. McPhail LD, Robinson SP. Intrinsic susceptibility MR imaging of chemically induced rat mammary tumors: relationship to histologic assessment of hypoxia and fibrosis. *Radiology* 2010; **254**: 110–8. doi: https://doi.org/10.1148/radiol.2541090395
78. Baker LC, Boult JK, Jamin Y, Gilmour LD, Walker-Samuel S, Burrell JS, et al. Evaluation and immunohistochemical qualification of carbogen-induced ΔR_2 as a noninvasive imaging biomarker of improved tumor oxygenation. *Int J Radiat Oncol Biol Phys* 2013; **87**: 160–7. doi: https://doi.org/10.1016/j.ijrobp.2013.04.051
79. Baker LCJ, Sikka A, Price JM, Boult JKR, Lepicard EY, Box G, et al. Evaluating imaging biomarkers of acquired resistance to targeted EGFR therapy in xenograft models of human head and neck squamous cell carcinoma. *Front Oncol* 2018; **8**: 271. doi: https://doi.org/10.3389/fonc.2018.00271
80. Little RA, Jamin Y, Boult JKR, Naish JH, Watson Y, Cheung S, et al. Mapping hypoxia in renal carcinoma with oxygen-enhanced MRI: comparison with intrinsic susceptibility MRI and pathology. *Radiology* 2018; **288**: 739–47. doi: https://doi.org/10.1148/radiol.2018171531
81. Price JM, Robinson SP, Koh DM. Imaging hypoxia in tumours with advanced MRI. *Q J Nucl Med Mol Imaging* 2013; **57**: 257–70.
82. Robinson SP, Rijken PF, Howe FA, McSheehy PM, van der Sanden BP, Heerschap A, et al. Tumor vascular architecture and function evaluated by non-invasive susceptibility MRI methods and immunohistochemistry. *J Magn Reson Imaging* 2003; **17**: 445–54. doi: https://doi.org/10.1002/jmri.10274
83. Howe FA, Robinson SP, Rodrigues LM, Griffiths JR. Flow and oxygenation dependent (FLOOD) contrast MR imaging to monitor the response of rat tumors to carbogen breathing. *Magn Reson Imaging* 1999; **17**: 1307–18. doi: https://doi.org/10.1016/S0730-725X(99)00089-2
84. Al-Hallaq HA, Zamora M, Fish BL, Farrell A, Moulder JE, Karczmar GS. MRI measurements correctly predict the relative effects of tumor oxygenating agents on hypoxic fraction in rodent BA1112 tumors. *Int J Radiat Oncol Biol Phys* 2000; **47**: 481–8. doi: https://doi.org/10.1016/S0360-3016(00)00445-4
85. Rodrigues LM, Howe FA, Griffiths JR, Robinson SP. Tumor R_2* is a prognostic indicator of acute radiotherapeutic response in rodent tumors. *Journal of Magnetic Resonance Imaging* 2004; **19**: 482–8. doi: https://doi.org/10.1002/jmri.20024
86. Taylor NJ, Baddeley H, Goodchild KA, Powell ME, Thoumine M, Culver LA, et al. BOLD MRI of human tumor oxygenation during carbogen breathing. *J Magn Reson Imaging* 2001; **14**: 156–63. doi: https://doi.org/10.1002/jmri.1166
87. Rijpkema M, Kaanders JHAM, Joosten FBM, van der Kogel AJ, Heerschap A. Effects of breathing a hyperoxic hypercapnic gas mixture on blood oxygenation and vascularity of head-and-neck tumors as measured by magnetic resonance imaging. *Int J Radiat Oncol Biol Phys* 2002; **53**: 1185–91. doi: https://doi.org/10.1016/S0360-3016(02)02825-0
88. Hoskin PJ, Carnell DM, Taylor NJ, Smith RE, Stirling JJ, Daley FM, et al. Hypoxia in prostate cancer: correlation of BOLD-MRI with pimonidazole immunohistochemistry-initial observations. *Int J Radiat Oncol Biol Phys* 2007; **68**: 1065–71. doi: https://doi.org/10.1016/j.ijrobp.2007.01.018
89. Alonzi R, Padhani AR, Maxwell RJ, Taylor NJ, Stirling JJ, Wilson JI, et al. Carbogen breathing increases prostate cancer oxygenation: a translational MRI study in murine xenografts and humans. *Br J Cancer* 2009; **100**: 644–8. doi: https://doi.org/10.1038/sj.bjc.6604903
90. Chopra S, Foltz WD, Milosevic MF, Toi A, Bristow RG, Ménard C, et al. Comparing oxygen-sensitive MRI ($BOLD_{R2*}$) with oxygen electrode measurements: a pilot study in men with prostate cancer. *Int J Radiat Biol* 2009; **85**: 805–13. doi: https://doi.org/10.1080/09553000903043059
91. Bayer C, Shi K, Astner ST, Maftei C-A, Vaupel P. Acute versus chronic hypoxia: why a simplified classification is simply not enough. *Int J Radiat Oncol Biol Phys* 2011; **80**: 965–8. doi: https://doi.org/10.1016/j.ijrobp.2011.02.049
92. Dewhirst MW. Relationships between cycling hypoxia, HIF-1, angiogenesis and oxidative stress. *Radiat Res* 2009; **172**: 653–65. doi: https://doi.org/10.1667/RR1926.1
93. Lanzen J, Braun RD, Klitzman B, Brizel D, Secomb TW, Dewhirst MW. Direct demonstration of instabilities in oxygen concentrations within the extravascular compartment of an experimental tumor. *Cancer Res* 2006; **66**: 2219–23. doi: https://doi.org/10.1158/0008-5472.CAN-03-2958
94. Baudelet C, Ansiaux R, Jordan BF, Havaux X, Macq B, Gallez B. Physiological noise in murine solid tumours using T2*-weighted gradient-echo imaging: a marker of tumour acute hypoxia? *Phys Med Biol* 2004; **49**: 3389–411. doi: https://doi.org/10.1088/0031-9155/49/15/006
95. Gonçalves MR, Johnson SP, Ramasawmy R, Pedley RB, Lythgoe MF, Walker-Samuel S. Decomposition of spontaneous fluctuations in tumour oxygenation using BOLD MRI and independent component analysis. *Br J Cancer* 2015; **113**: 1168–77. doi: https://doi.org/10.1038/bjc.2015.270
96. Panek R, Welsh L, Baker LCJ, Schmidt MA, Wong KH, Riddell AM, et al. Noninvasive imaging of cycling hypoxia in head and neck cancer using intrinsic susceptibility MRI. *Clin Cancer Res* 2017; **23**: 4233–41. doi: https://doi.org/10.1158/1078-0432.CCR-16-1209
97. Chaplin DJ, Durand RE, Olive PL. Acute hypoxia in tumors: Implications for modifiers of radiation effects. *Int J Radiat Oncol Biol Phys* 1986; **12**: 1279–82. doi: https://doi.org/10.1016/0360-3016(86)90153-7
98. Dewhirst MW, Kimura H, Rehmus SW, Braun RD, Papahadjopoulos D, Hong K, et al. Microvascular studies on the origins of perfusion-limited hypoxia. *Br J Cancer Suppl* 1996; **27**: S247–51.
99. Zhou H, Hallac R, Yuan Q, Ding Y, Zhang Z, Xie X-J, et al. Incorporating oxygen-enhanced MRI into multi-parametric assessment of human prostate cancer. *Diagnostics* 2017; **7**: 48. doi: https://doi.org/10.3390/diagnostics7030048
100. Jones KM, Michel KA, Bankson JA, Fuller CD, Klopp AH, Venkatesan AM. Emerging magnetic resonance imaging technologies for radiation therapy planning and response assessment. *Int J Radiat Oncol Biol Phys* 2018; **101**: 1046–56. doi: https://doi.org/10.1016/j.ijrobp.2018.03.028